Morphological Partitioning of Ethyl Branches in Polyethylene by ^{13}C Nuclear Magnetic Resonance

E. Pérez† and D. L. VanderHart*

Polymers Division, National Bureau of Standards, Gaithersburg, Maryland 20899

Buckley Crist, Jr., and P. R. Howard

Materials Research Center, Northwestern University, Evanston, Illinois 60201.
Received June 12, 1986

ABSTRACT: A combination of ^{13}C and ^{1}H magnetic resonance experiments has been performed on a model ethylene copolymer (hydrogenated polybutadiene) of about 100 000 molecular weight and 17 ethyl branches per 1000 total carbons. The fraction of ethyl branches found in the crystal in this 41% crystalline sample was 0.06 ± 0.02, and the ratio of concentrations between the crystalline and noncrystalline regions was correspondingly about 1:10. For reasons of best integrability, the methyl resonance of the ethyl branches was used to deduce the concentrations in each morphological phase. This same resonance is rather ill-behaved in cross-polarization experiments, so several auxiliary experiments were undertaken to deduce the true concentrations attributed to each phase. The experimental technique utilizes cross-polarization as a probe of proton polarization levels; moreover, the success of the method relies on local proton spin diffusion. Results are discussed in terms of other experimental findings regarding the question of partitioning. Also, these results are used to interpret more accurately the data in a previous report on partitioning in an ethylene–1-butene copolymer having a branch concentration about 7 times smaller. Finally, in an appendix, some supplemental data are presented on the effects of magic-angle spinning on the spin dynamics of the noncrystalline region and the influence of this spinning on the validity of the results deduced from cross-polarization experiments.

Introduction

One of the topics in the crystallization of polymers that has been the subject of a great number of publications (and controversy) is the incorporation of chain defects (end groups, branches, or comonomer units) in the crystal lattice of polyethylene (PE). While some theories have been based on the total exclusion of defects from the lattice,[1,2] the expansion of the unit cell in solution-crystallized[3,4] and bulk-crystallized branched polyethylenes[5–13] and other copolymers has been taken as proof of the inclusion of branches in the crystal, although other factors such as crystal thickness[14–16] may influence this expansion.

Studies of the melting point behavior of ethylene copolymers possessing different kinds of branches[14,16] conclude that methyl branches enter the lattice under equilibrium conditions while other kinds of branches are present only as nonequilibrium defects, which, in turn, cause a lowering of the melting temperature independent of the chemical nature of the side group.[16] This melting point lowering has a strong dependence on the branch distribution as well as on the average concentration of branches.

Determinations of the partitioning of vinyl end groups in solution crystals of PE have been reported,[17–20] and several attempts have also been made[12,21–23] to establish whether branches are included in the crystals in bulk-crystallized PE. Virtually all previous studies have been handicapped because they relied on experimental observations that were qualitatively interpretable at best. For example, the amount of lattice expansion or enthalpy defect resulting from the incorporation of an ethyl branch in a PE crystal is not known. Similarly, the exact reduction in crystallinity and crystal thickness caused by strict exclusion of branch points has not been calculated for real semicrystalline copolymers. Additional complications can arise if there are uncertainties about the type of chain defects present and, more importantly, their distribution along the chain.

In this paper we ask whether an ethyl branch exists within or outside a crystalline region; i.e., are the surrounding backbone chain segments predominantly crystalline or predominantly noncrystalline? Whether a branch fits neatly into the crystal or gives rise to a major defect is a peripheral concern. Furthermore, in recognition of the importance of the interferace between crystalline and noncrystalline regions, particularly in copolymers,[16,24] we will consider whether there is any indication that the branches are concentrated at the interface.

This study is done with a solid-state NMR method developed very recently[25] for measuring the crystalline/noncrystalline partitioning of defects and for establishing the concentrations of different kinds of defects in each phase. The method is based on the uniformity of proton polarization in the immediate vicinity of a defect and on the spectral isolation of defect resonances; the method also relies on the solid-state ^{13}C techniques of cross-polarization (CP),[26,27] high-power proton decoupling,[28,29] and magic-angle sample spinning (MAS).[30,31]

In the original report,[25] methyl ends, vinyl ends, and ethyl branches were studied in an ethylene–1-butene copolymer (E/B). The partitioning of both types of chain ends was established; however, substantial ambiguity existed in the case of the ethyl branches. The ambiguity stemmed from ethyl methyl ($1B_2$) signals which, in CP, were too weak. There was also a question whether all of the $1B_2$ carbons give rise to relatively narrow resonances. The possibility was entertained that a $1B_2$ carbon in a crystalline environment could be sufficiently constrained so that the motion of this ethyl group would cause its resonance to become broadened to the point of undetectability.[25]

The purpose of this paper is to establish the amount of ethyl branches included in the crystal in a sample of hydrogenated polybutadiene (HPB) by using ^{13}C NMR in the solid state. The questions about the $1B_2$ resonances in the foregoing paragraph will be resolved principally because the concentration of ethyl branches is about an order of magnitude higher in this sample than it was in the E/B sample. The higher concentration of branches gave the needed sensitivity increase for characterizing $1B_2$ signal

†Present address: Instituto de Plásticos y Caucho, Juan de la Cierva 3, 28006-Madrid, Spain.

0024-9297/87/2220-0078$01.50/0

more quantitatively, particularly in CP experiments.

Experimental Section

The NMR spectrometer employed in this study is a Bruker CXP200,[32] which operates at a magnetic field of 4.7 T; the ^{13}C frequency is 50.3 MHz. The MAS probe was manufactured by Doty Scientific.[32] The pulse sequences employed and their rationale in the context of this problem have been discussed previously.[25] Typical radio frequency field strengths were set to yield precession frequencies of about 70 kHz, although the proton and carbon radio frequency precession frequencies differed by the spinning frequency (about 3 kHz) so that CP rates would be optimized.[33] The high-resolution solution-NMR determination of the ethyl branch content was carried out on a Bruker WM400[32] spectrometer operating at 9.4 T. The spectrum was taken at 120 °C in a 15% by weight solution in 1,2,4-trichlorobenzene. Other parameters used in this acquisition are outlined in the literature.[34]

The HPB sample was synthesized at Northwestern University by established procedures.[35] Other publications[36,37] describe the distribution of branches and the preparation of similar samples as well as some morphological characteristics.[24] According to the polymerization conditions, the mole fraction of vinylene additions is expected to be in the range 0.075 ± 0.010; high-resolution NMR analysis verifies this, as will be shown later. The important aspect of HPB for this work is that it is a linear polymer containing only ethyl branches. These are distributed along the chain in a manner expected for a random copolymer of ethylene and 1-butene having the same overall branch concentration.[37] The weight-average molecular weight of this sample is 115000, and the polydispersity is less than 1.1. These characteristics were chosen so that chain-end resonances would be so weak that they would not interfere with any of the resonances of interest.

The crystallization of this sample was carried out by compression molding a cylindrical plug starting in the melt at 135 °C and slowly cooling at about 1 °C/min to 70 °C. The crystallinity was not measured directly by a technique other than NMR; however, results on similarly branched samples yield crystallinities on the range 0.35–0.45 based on density.[17,38] Crystallinity in samples such as these is not very sensitive to thermal history.[24] On the basis of a crystallographic density ρ_c = 0.986 g/cm^3 measured for a comparable HPB,[39] the weight fraction crystallinity is calculated as 0.45.

Small-angle X-ray scattering was performed on a 1-mm-thick slice of the NMR-analyzed specimen. The X-ray instrument used Cu Kα radiation, pinhole collimation, and a one-dimensional position-sensitive detector. The data were also corrected for background scattering following the measurement of the absorption coefficient. Rat-tail tendon (collagen) was used to calibrate the system. The peak in the corrected data appeared at a distance corresponding to a 19-nm-long spacing. A Lorentz correction was then applied to this data, and the Lorentz-corrected peak position indicated a long spacing of 13 nm, within 13% of the value seen previously.[39]

Results

A. Outline of the Arguments for Determining Partitioning. The determination of ethyl branch partitioning involves several experiments, many of which were necessitated because the $1B_2$ resonance is easiest and least ambiguous to integrate, yet it is ill-behaved as a resonance in CP experiments. The average branch concentration was determined by solution-state ^{13}C NMR. Then, by use of Boltzmann populations, the true NMR crystallinity, based on ^{13}C resonance separation, was measured. It was also verified by comparison of signal intensity with a standard sample that within experimental error, all of the backbone carbons were observable; i.e., they were not excessively broadened by molecular motion. A comparison of the Boltzmann intensity between the $1B_2$ and the backbone carbons indicated that the $1B_2$ signal was also well-behaved; i.e., no portion showed excessive broadening. The CP spectra (1-ms CP time) were taken in the usual way[25] following different preparations of proton magnetization, and linear-combination spectra were formed in order to isolate the "pure crystalline" and "pure noncrystalline" spectra. The pure crystalline spectrum indicated that a weak, downfield shoulder in the $1B_2$ resonance was associated with the crystalline regions, while the pure noncrystalline spectrum showed the $1B_2$ resonance to be at 11.3 ppm. The apparent ethyl branch concentration ratio in these pure spectra was 1:7 for the crystalline and noncrystalline components, respectively. Since the total concentration of ethyl branches implied by the two pure CP spectra fell considerably short of the known average branch concentration, the remaining experimental effort was focused on assigning the intensity deficiency to the appropriate morphological component(s) so that true concentration ratios could be obtained. A part of this effort was to show that the $1B_2$ carbons in the downfield (crystalline) shoulder experience a stronger local proton dipolar field compared with their upfield (noncrystalline) counterparts. This stronger field is what is expected if the branch resides in a less mobile (crystalline) environment. Measurements of signal strength as a function of CP time and with a 10-kHz Hartmann–Hahn mismatch demonstrated this claim. The variable CP time experiments also demonstrated that after 1-ms CP time the apparent ethyl branch concentration in the pure crystalline spectrum would be close to the true concentration. The Hartmann–Hahn mismatch experiments, because they discriminate strongly against the noncrystalline $1B_2$ signal, also showed more clearly than in the other experiments that the $T_{1\rho}^H$ values for the $1B_2$ protons in each phase mirror very well the $T_{1\rho}^H$ behavior of the corresponding backbone protons. This latter experiment also suggests that the crystalline ethyl branches are distributed throughout the crystalline phase and not concentrated at the crystal/noncrystal interface. The distribution of branches in each phase will be considered briefly in the Discussion section in the light of these data.

B. Determination of Branch Concentration via Solution ^{13}C NMR. A 9.4-T ^{13}C NMR spectrum of the HPB indicated that the true average concentration of ethyl branches in this sample is 17.4 ± 0.5 per 1000 total carbons. This number is in good agreement with the concentration expected on the basis of previous work[35] and the polymerization conditions.

C. Determination of Crystallinity and Verification That No Ethyl Methyl Signals Are Excessively Broadened. In order to determine the crystallinity of this sample and to verify that all of the $1B_2$ resonances were well-behaved (not excessively broadened by motion), T_1^C measurements were performed by using the saturation–recovery, $(90° - t)_x$, method. This method was further modified by a 3-s delay between observation and saturation. This delay allowed the protons to recover their Boltzmann populations so that no transient Overhauser[40] distortions were present at short t values. This method is much more tedious than the method of Torchia,[41] but by avoiding CP, we avoided the problem of distorted CP intensities.

Figure 1 shows the approach of ^{13}C relative intensities toward their equilibrium intensities as a function of t for the various distinguishable lines in the spectrum. Figure 2 shows spectra having t values of 5 and 800 s. T_1^C values deduced from Figure 1 for the methine, $1B_2$, and noncrystalline backbone methylene carbons are respectively 0.30 ± 0.10, 0.60 ± 0.10, and 0.25 ± 0.04 s. The decay of the crystalline methylene carbon magnetization is not exponential, a normal finding,[42-44] and the long T_1^C associated with approximately 65% of this signal is 120 s. This is a relatively short crystalline relaxation time for PE,[42] and it indicates that the crystals are either relatively thin

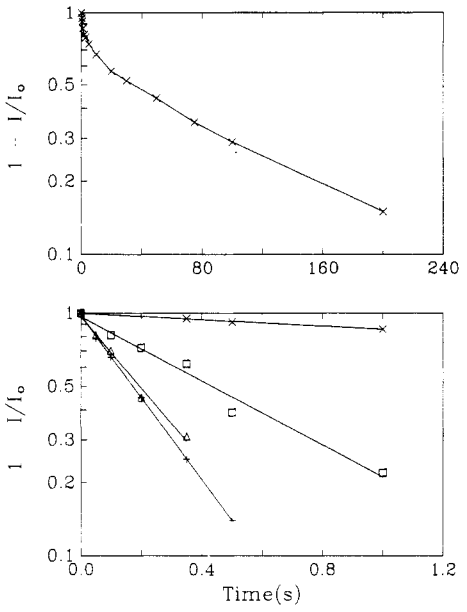

Figure 1. Approach of the different Zeeman magnetizations toward equilibrium in HPB in a saturation–recovery experiment. The upper curve represents only crystalline magnetization and extends to long times. The lower family of curves for short times gives the behavior of the following carbon magnetizations: noncrystalline backbone (+); crystalline backbone (×); methine (△); and $1B_2$ (□). The methine and noncrystalline backbone carbons behave very similarly, suggesting that most branches are outside the crystalline regions. In the upper curve, the solid line simply joins the experimental points. In the lower curves, the solid line is the best least-squares straight-line fit to the data.

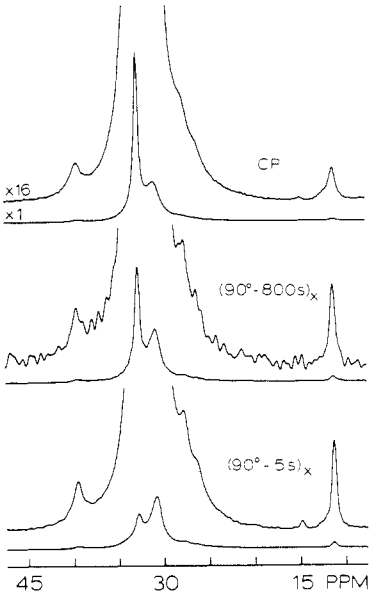

Figure 2. HPB spectra taken under the indicated conditions. Both a ×1 and ×16 amplification factor apply to each spectrum. The CP spectrum is 5000 scans with a 1-ms CP time and 7 s between pulses. The $(90° - 800\ s)_x$ and $(90° - 5\ s)_x$ are saturation–recovery spectra representing 200 and 10 000 scans, respectively. The $(90° - 800\ s)_x$ spectrum represents the equilibrium Boltzmann signal for all the carbons. This spectrum is a reference for the other two: the CP spectrum has the same total intensity and the $(90° - 5\ s)_x$ spectrum is normalized to the same number of scans. Note the distortion of the crystallization/noncrystalline relative intensities in the CP spectrum and the full recovery of the noncrystalline signal after 5 s in the $(90° - 5\ s)_x$.

or contain defects which produce greater mobility. The $(90° - 5\ s)_x$ spectrum of Figure 2 represents fully relaxed intensities for all but the crystalline backbone carbons and the $(90° - 800\ s)_x$ experiment represents the whole equilibrium signal. For comparison, a CP spectrum obtained with a 1-ms CP time is also shown in Figure 2, normalized to the same total intensity as the $(90° - 800\ s)_x$ spectrum. It is clear from these two latter spectra that substantial distortions in the relative intensities of the crystalline (32.9 ppm) and noncrystalline (31.1 ppm) backbone resonances exist; moreover, the CP intensities of the methine (39.8 ppm) and the $1B_2$ (11.3 ppm) resonances are also significantly reduced relative to their true values. For the 1-ms CP time, the CP enhancement factors, relative to their Boltzmann intensities are 3.2, 1.6, 1.6, and 1.1 for the 32.9, 31.1, 39.8, and 11.3 ppm peaks, respectively. The true values of the branch intensities may be seen more clearly in the $(90° - 5\ s)_x$ spectrum of Figure 2 because of the larger number of scans compared with the $(90° - 800\ s)_x$ spectrum.

The $(90° - 800\ s)_x$ experiment of Figure 2 was used to determine the true NMR crystallinity, 0.41, for the sample. This agrees quite well with the crystallinity of 0.45 from density. The functional definition of a crystalline region in this paper is that the resonance of a ^{13}C nucleus in such a region appears in the 32.9 ppm band. The fact that the T_1^C behavior within this band is not single-exponential (see Figure 1) implies that mobility is not entirely uniform throughout this crystalline region. It is likely that included in this definition of crystallinity is at least a part of the crystalline/noncrystalline interface. While at least some of those crystalline carbons with shorter relaxation times may be in the vicinity of a "crystalline branch" and thus acquire more mobility, this is not the entire explanation since even melt-crystallized linear high-density polyethylenes show this more mobile crystalline fraction.[44,45]

In the $(90° - 5\ s)_x$ spectrum of Figure 2 evidence of other carbon resonances associated with ethyl branches may be seen at 27.9 and 26.3 ppm. These resonances are respectively associated with the β-methylene backbone carbons and the ethylmethylene carbon ($2B_2$), in analogy with the solution measurements.[34,46-48]. Although not very apparent in the spectra of Figure 2, the resonance of the backbone methylene carbon attached to the methine is also visible at 34.2 ppm if resolution enhancement is used in Fourier transforming the $(90° - 5\ s)_x$ spectrum. While one would like to use all of these resonances in studying the partitioning of branches, this is not possible. Only the methine and $1B_2$ resonances are well enough separated from the dominant backbone resonances for integration. The methine resonance, however, overlaps the main peak sufficiently that the choice of base line is somewhat arbitrary. Therefore, only the $1B_2$ resonance is considered to be sufficiently removed from the other resonances to be integrable on an absolute basis. This is, in many ways, unfortunate because the methine carbons have more efficient CP than the $1B_2$ carbons and, therefore, would be easier to base partitioning arguments on, were it not for the integration problem. One favorable aspect is that the $1B_2$ resonance is distinct from the chain-end methyl at 15 ppm; this latter resonance is weak in the spectra of Figure 2 because the number-average molecular weight is about 100 000. At the same time, the intensity of the resonance is 2–3 times higher than would be expected for this molecular weight.

In order to determine whether carbon resonances from all of the $1B_2$ sites were well-behaved, i.e., not excessively broadened, the integral of the fully relaxed $1B_2$ peak in the $(90° - 5\ s)_x$ experiment was compared to the total integral in the $(90° - 800\ s)_x$ experiment. This ratio gave a total concentration of ethyl branches of 17.2 ± 0.7 per 1000 total carbons. The corresponding attempted inte-

gration of the methine resonance gave only 13.4 ± 2.0 branches per 1000 carbons. Thus, either some of the branch resonance is broadened, or some branch intensity is shifted into the main peak and obscured, or the base line for integration is not correctly chosen because of partial overlap with the backbone resonances. The latter is the most likely choice, but the other choices cannot be discounted. The agreement of the $1B_2$ intensity with expectations based on solution results indicates that all of the $1B_2$ intensity is observable; i.e., no significant $1B_2$ intensity is excessively broadened by molecular motion. Since this latter claim depends on the assumption that none of the backbone resonances are excessively broadened either, the signal strength per carbon in the $(90° - 800\ s)_x$ experiment was compared with the corresponding quantity in an adamantane sample having a nearly identical filling factor. Agreement was within experimental error, i.e., less than 4% deviation; therefore, neither the $1B_2$ nor the backbone methylene resonance is excessively broadened.

The T_1^C relaxation of the methine resonance in Figure 1 closely parallels that of the noncrystalline methylene resonance. The fact that the methine carbon is part of the backbone might thus imply that most ethyl branches are in the noncrystalline region. However, if the ethyl branch in a crystalline environment exists as a major local defect, there could be enough conformational mobility at this site to allow the methine to relax efficiently. Thus, the methine T_1^C cannot be used as conclusive proof of the location of the branches.

D. Partitioning of the Ethyl Branches. The principal argument for determining the partitioning of branches between the crystalline and noncrystalline region is based on the method outlined in a previous paper.[25] There it was argued that on a very local scale (less than 1 nm), the protons, even those on a chain end or on a branch, are very close to "spin equilibrium" with their nearest-neighbor protons belonging to backbone methylene groups. By spin exchange or spin diffusion among the protons, therefore, the average polarization of each proton, even those on branches or other small defects, is locally quite uniform. On the other hand, over much larger distances of, say, 5–20 nm, which is the scale of morphological variations, proton polarization gradients could exist because spin diffusion over such lengths requires more time. Thus, in a $T_{1\rho}^H$ experiment, the average noncrystalline proton signal will typically decay faster than the crystalline signal; this reflects gradients on a scale of the morphological variations. Locally, however, protons associated with chain ends or branches, even though they may possess intrinsic $T_{1\rho}^H$ values distinct from backbone methylene protons, will have apparent $T_{1\rho}^H$ values close to those of the protons in the phase in which these defects are embedded. This is the fundamental mechanism for distinguishing between resonances originating from different morphological phases. Serious problems for the partitioning method could arise when the intrinsic $T_{1\rho}^H$ of the ethyl protons approaches the $T_{1\rho}^H$ minimum of about 0.1 ms. It is exceedingly unlikely that this situation prevails here since excessive line broadening is not present in the $1B_2$ carbon peak.

In CP experiments employing any fixed CP time, the ^{13}C nuclei serve as a probe of proton polarization. The ^{13}C resonances associated with a particular concentration of defects in one morphological phase will have an intensity proportional to the intensity of the backbone methylene carbon resonance of that morphological phase. In the simplest case, the ratio of defect to backbone intensities gives us the defect concentration in that phase. However, possible differences in molecular mobility associated with defects and with different backbone environments may be reflected in different CP efficiencies, thus causing distortions in relative intensities for different kinds of carbons within a given phase. Since line widths and relaxation times of protons in the crystalline and noncrystalline regions differ in PE, states of proton polarization may be prepared in which proton polarization gradients exist between the crystalline and noncrystalline regions. Therefore, CP spectra representing different mixtures of crystalline and noncrystalline ^{13}C backbone intensities can be generated. The basis of the method then is that one collects ^{13}C spectra, three in the present case, using a fixed CP time and a variable preparation of proton polarization. By suitable linear combinations of these spectra, one can isolate the respective crystalline and noncrystalline backbone resonances. Then, because of the proportionality characteristic just mentioned, one can at the same time isolate the defect resonances existing in either the crystalline or the noncrystalline region.[25] The only problem is that the ratios of intensities between the backbone and defect resonances in a given phase need not yield directly the true concentrations of defects since CP efficiencies for the defect and the backbone carbons may differ. If the latter situation prevails, as will be seen for the $1B_2$ resonance, the apparent concentration will be a function of the CP time selected. Full analysis of the signal amplitudes in polyethylene as a function of CP time does not, by itself, yield true concentrations. Reasons for this are given in the Appendix.

Table I
Relative Intensities and Line-Shape Analysis for the Different Spectra

expt	area per scan[a]	crystal area[a,b]	noncrystal area[a,b]	apparent crystal content
CP	6.07	3.60	2.51	0.59
SL4 + CP	2.85	2.08	0.77	0.73
DE5 + CP	1.59	0.11	1.48	0.07
$(90° - 5\ s)_x$	1.97	0.32	1.65	0.16
$(90° - 800\ s)_x$	2.80	1.15	1.65	0.41

[a] In arbitrary units. [b] Based on the pure component line shapes.

The three different CP experiments used were very similar to those reported earlier for the E/B sample.[25] The rationalization for each preparation of proton polarization will not be repeated here. A few adaptations were required, however, because of the lower crystallinity and the shorter $T_{1\rho}^H$ values of 8.7 and 4.0 ms respectively for the crystalline and noncrystalline proton resonances encountered in the HPB sample. A 1-ms CP time was chosen, as before. The first experiment, "CP", was the usual CP experiment. The second, called "SL4 + CP", involved a 4-ms proton spin-locking period prior to CP. The third experiment, "DE5 + CP", included a preparation of five dipolar echoes[49] (2τ = 24 μs) prior to CP. These three spectra are shown in Figure 3, each normalized to the same total intensity. Total CP intensities per scan and the apparent crystalline and noncrystalline contributions to each line shape are summarized in Table I.

From these, three linear-combination spectra for the pure crystalline line shape were generated; three other spectra corresponding to the noncrystalline spectrum were also obtained. The average of each of these was designated the "pure crystalline" and "pure noncrystalline" spectrum. These are shown in Figure 4, where each is normalized to the same total intensity. It is immediately obvious that the intensity of the $1B_2$ peak is much larger in the pure noncrystalline spectrum, indicating that most of the

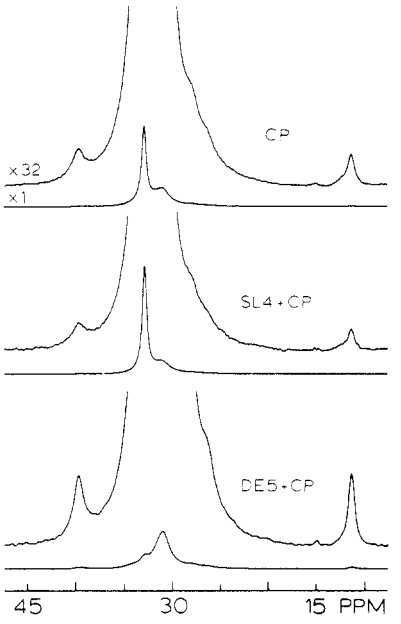

Figure 3. CP spectra of HPB at two amplification factors (×1 and ×32). Each spectrum is normalized to the same total intensity so that comparison may be made on the basis of concentrations. The labels are explained in the text. The differing ratios of crystalline (32.9 ppm) and noncrystalline (31.1 ppm) backbone intensities in each spectrum provide the basis for taking linear combinations of these spectra in order to isolate the pure crystalline and pure noncrystalline signals in Figure 4. The CP time was 1 ms, and the number of scans was 5000, 9600, and 20 000 in the upper to lower spectra, respectively.

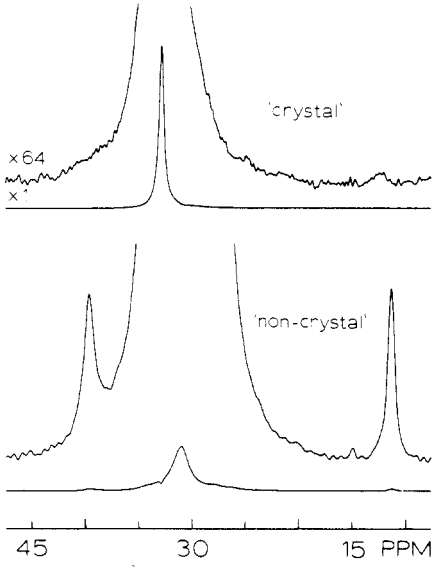

Figure 4. Pure crystal and pure noncrystal spectra generated from linear combinations of the spectra of Figure 3 (see text). They are normalized to the same total intensity, and amplification factors are the same for each spectrum. Weak branch resonances, both methine and $1B_2$, are still visible in the upper spectrum. Note that the $1B_2$ peak is shifted downfield compared to the $1B_2$ resonance in the lower spectrum.

branches are found in the noncrystalline region. The apparent concentrations in the crystalline and noncrystalline regions are 2.7 ± 0.7 and 17.9 ± 1.3 branches per 1000 total carbons in each phase. This leads to an apparent average concentration of 11.7 ± 1.1 branches per 1000 total carbons, which is well short of the 17.4 branches known to exist in the sample. Even though this discrepancy exists, the following very plausible statements may be made. First, the most likely source of the above discrepancy is that substantial mobility exists at the noncrystalline $1B_2$ sites,

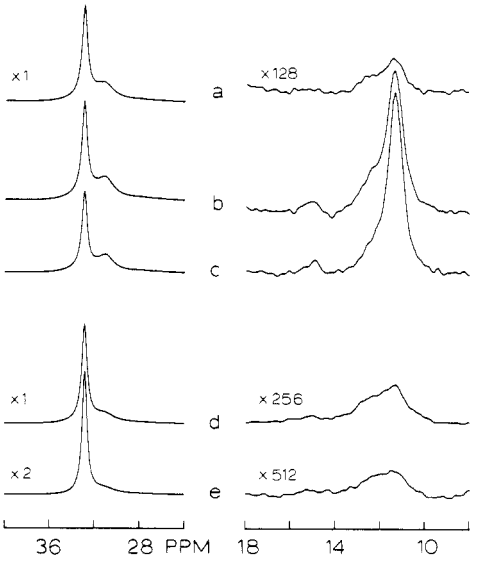

Figure 5. HPB spectra which reinforce the idea that the $1B_2$ carbon intensity at 12.3 ppm can be associated with crystalline branches. All spectra show the backbone and $1B_2$ carbon regions. Amplification factors, if not given, are the same as in the spectrum above. All spectra represent 20 000 transients and are normalized to the same total number of scans. Spectra a, b, and c are CP spectra, corresponding to CP times of 0.2, 1, and 3 ms, respectively. Note that the 12.3 ppm shoulder cross-polarizes more quickly than the 11.3 resonance, thereby indicating a stronger dipolar field or a more rigid molecular environment around the carbons resonating at 12.3 ppm. Spectra d and e and CP spectra taken with a 0.7-ms CP time and a 10-kHz mismatch of the Hartmann–Hahn condition away from optimum. Spectra d and e differ in that a spin-lock time of 0.1 and 5 ms, respectively, preceded the CP. The $T_{1\rho}{}^{H}$ of the 12.3 ppm shoulder deduced from deconvolution of the $1B_2$ region of spectra d and e agrees with the $T_{1\rho}{}^{H}$ for the crystalline carbons.

causing a reduction of proton–carbon dipolar fields and a consequent lowering of the CP efficiency for these carbons relative to the noncrystalline backbone carbons. Second, any $1B_2$ carbons within a crystalline region will be much less mobile than their noncrystalline counterparts; therefore, the local proton–carbon dipolar fields should be stronger, so CP efficiencies should be higher. Third, it is thus reasonable that the CP $1B_2$ intensity associated with the "true crystalline" line shape will give the true crystalline $1B_2$ concentration, while the pure noncrystalline line shape will underestimate the true $1B_2$ concentration. If the above statements are true and if the noncrystalline concentration is increased to be consistent with the known average concentration of branches and the known crystallinity, then the noncrystalline concentration becomes 27.6 per 1000 total carbons compared with the 2.7 per 1000 carbons in the crystalline region. We will now justify this modification of the $1B_2$ concentration in the noncrystalline phase.

Since the spectra of Figure 4 indicate that the crystalline $1B_2$ carbons are shifted by 1 ppm downfield from the noncrystalline $1B_2$ carbons, one would like to take advantage of the spectral separation and reinforce the assignment of the 12.3 ppm peak to the crystalline region by showing that the carbons in this downfield shoulder experience a stronger local proton dipolar field than their 11.3 ppm noncrystalline counterparts. To this end, two sets of experiments were performed, some results of which are shown in Figure 5. Spectra 5a, 5b, and 5c show the backbone and $1B_2$ signals as a function of the CP times, 0.2, 1, and 3 ms, respectively. It is clear, particularly in spectrum 5a, that the downfield shoulder cross-polarizes more efficiently than the main upfield portion of the $1B_2$

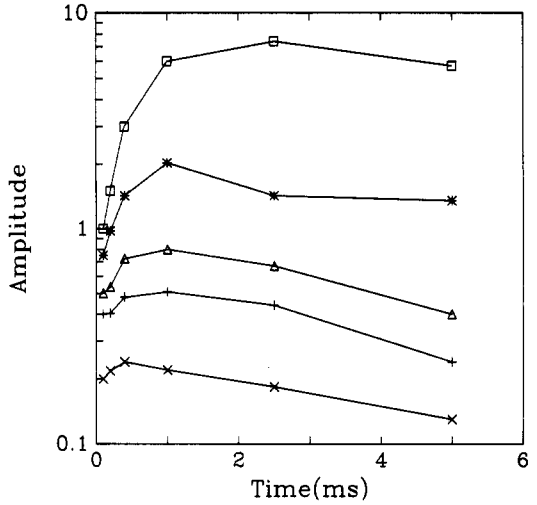

Figure 6. CP intensities (on arbitrary scales) of various lines in HPB as a function of CP time. The carbon lines and symbols have the following correspondence: crystalline backbone (×); noncrystalline backbone (+); methine (△); crystalline $1B_2$ at 12.3 ppm (*); and noncrystalline $1B_2$ (□). Note that the latter carbon line is the most sluggish in CP behavior.

line, implying a larger proton dipolar field for the former carbons, as is expected for nuclei in the crystalline regions. The CP intensities of the backbone carbons and the branch carbons are plotted in Figure 6 as a function of CP time between 0.1 and 5 ms. For Figure 6 an attempt was made to deconvolute the $1B_2$ resonance and to follow the growth of each part of the line separately. Errors in the 12.3 ppm amplitude are quite large, particularly at the longer CP times since separation from the increasingly dominant 11.3 ppm resonance becomes more arbitrary.

The second set of experiments, to enhance the 12.3 ppm $1B_2$ resonance relative to the 11.3 ppm peak, utilized a Hartmann–Hahn mismatch of about 10 kHz with proton spin-locking for 0.1 or 5 ms preceding a 0.7-ms CP time. The corresponding backbone and $1B_2$ peaks (with different amplification factors) are shown in Figure 5d,e. The loss of intensity for the 11.3 ppm peak was much more severe than for the 12.3 ppm peak. From Figure 5d,e, $T_{1\rho}{}^H$ values were estimated for the 12.3 ppm shoulder and the 11.3 ppm peak as well as for the backbone resonances at 32.9 and 31.1 ppm. These values are 8.2 ± 1.3, 3.7 ± 0.6, 8.7 ± 0.3, and 4.0 ± 0.2 ms, respectively. Even though the errors associated with the $1B_2$ resonances are substantially larger than the errors in the backbone resonances, three conclusions may be drawn. First, the 12.3 ppm peak can be associateed with the crystalline region because its $T_{1\rho}{}^H$ value agrees with that of the backbone carbons in the crystalline regions. Second, this agreement of the $T_{1\rho}{}^H$ values for the protons near the 12.3 ppm carbons and the protons attached to the backbone crystalline carbons indicates that the crystalline ethyl branches are not likely to be concentrated near the crystal/noncrystal interface. If they were, the $T_{1\rho}{}^H$ value deduced from the 12.3 ppm peak would be more intermediate between the $T_{1\rho}{}^H$ values for the crystalline and noncrystalline backbone protons. Third, since the mismatch experiment could have preferentially selected any 11.3 ppm intensity having larger-than-average local proton dipolar fields, some of which intensity could conceivably be associated with the crystalline regions, the presence of such intensity would be indicated by a $T_{1\rho}{}^H$ longer than the $T_{1\rho}{}^H$ of the noncrystalline backbone protons. This was not found; therefore, the conclusion drawn from the pure crystalline spectrum that the crystalline $1B_2$ carbons only resonate at 12.3 ppm is supported.

Because the 12.3 ppm $1B_2$ carbons experience a stronger proton dipolar field and have greater CP rates compared with the 11.3 ppm carbons and because the CP intensity maximum occurs at 1 ms (see Figure 6), the concentration of ethyl branches in the crystalline phase is well approximated by the apparent concentration deduced from the pure crystalline spectrum of Figure 4.

We conclude that the concentration ratio of ethyl branches in the crystalline and noncrystalline regions is about 1:10 and the total fraction of branches in the crystalline region is 0.06 ± 0.02 (2.7 × 0.41/17.4) in this 41% crytalline HPB sample. Additional proof of this thesis is that a shoulder compromising about 8% of the total $1B_2$ intensity is consistent with the $(90° - 5\ s)_x$ $1B_2$ line shape (Figure 2).

Discussion

The concentration ratio of ethyl branches in the crystalline vs. the noncrystalline regions indicates that branch incorporation into the crystal is not energetically favored. That 4%–8% of the total branches are found in the crystal may well explain the unit-cell expansion observed for branched polyethylenes.[5-13] Much experimental evidence can be cited for the role that ethyl branches play in reducing crystallinity, so it is no surprise that most of the ethyl branches are in noncrystalline environments. But the existence of ethyl branches in the crystalline region raises the question whether such branches are an expression of an equilibrium or a nonequilibrium system. We will not speculate on whether much slower rates of crystallization would result in a greater exclusion of branches from the crystalline regions. It is known, however, that total crystallinity is not very sensitive to crystallization conditions for this level of branches.[24]

On the basis of the melting behavior of various copolymers,[14,16] it has been argued that only methyl branches go into the lattice under equilibrium conditions. Other types of branches including ethyl, propyl, hexyl, and acetate branches go into the lattice as nonequilibrium defects and invariably cause a lowering of the melting temperature, independent of the chemical nature of the branch.[16] It has also been observed[8,43] that as crystallization conditions depart from the high-temperature isothermal regime, more and longer branches may be incorporated into the crystals.

A related point of view is offered by Vonk and Pijpers,[21] who have analyzed crystal perfection and crystallinity reduction parameters. They conclude that there are two categories of branches: small groups like methyl branches that fit into the lattice in an interstitial way, and larger branches that require extensive chain rearrangement in order to fit into the lattice. In their view, the ethyl branches possibly occupy an intermediate position between these extremes. Seguela et al.[50] have considered the likelihood of ethyl branches being incorporated in interstitial sites and have concluded that such a mode is not favored. Their viewpoint leads to the prediction that ethyl branches ought to be excluded from the crystalline regions to a much greater extent than methyl branches. We have preliminary data on a methyl-branched PE which indicates that methyl groups are indeed more numerous in the crystalline regions compared with ethyl branches. These data will be reported in a forthcoming paper.

An additional feature is the experimental observation that both unit-cell expansion[6,43] and melting point depression[16] depend rather strongly on the distribution of the branches. The more random the distribution, the more pronounced are the effects. The HPB used in this study is a nearly randomly branched polymer.[16,37]

Several attempts[12,21-23] have been made in the literature to establish the partitioning of branches. The work of Holdsworth and Keller[23] on nitric acid etching of single crystals of a branched polymer with radioactive ethyl branches is particularly noteworthy. In their work, they found that about 5% of the ethyl branches remained in the crystalline residue following 72 h of nitric acid etching. So even in solution-grown crystals and even with possible questions whether the method rigorously captures the original crystalline state, ethyl branches remained. The levels that they found in these solution-grown crystals we consider to agree quite well with our findings for bulk-crystallized HPB. This agreement stands in contrast to the large differences we reported for vinyl end-group partitioning[25] in bulk-crystallized PE vs. the reported partitioning in single crystals.[17-20]

The authors of a very recent article[51] in which ^{13}C MAS techniques were employed also came to the conclusion that most of the ethyl branches are in noncrystalline regions in an E/B copolymer. These authors made no attempt to be quantitative; moreover, our work is not in total agreement with some of the assumptions made by those authors in interpreting their spectra.

Part of our motivation for undertaking this work was to understand better the results of our work on the E/B copolymer, particularly as regards the partitioning of the ethyl branches. In that study we encountered the problem of weak $1B_2$ intensities in the CP spectra, and the sensitivity was insufficient to investigate the problem in detail. From the present study, however, we can extrapolate to the E/B system and argue that all of the $1B_2$ resonance is well-behaved and not excessively broadened at room temperature. Therefore, there is no need to make allowance for possible crystalline branches, based on what was not seen. Since the pure crystalline spectrum in that work showed no observable signal in the $1B_2$ region, the upper limit for the crystalline concentration thus becomes 0.26 branches per 1000 crystalline carbons (the sensitivity limit). If the remaining carbons in the known average concentration are then placed in the noncrystalline region, which comprised 24% of that sample, then the concentration of noncrystalline branches is 10.2 per 1000 noncrystalline carbons. In other words, the branch concentration ratio between the crystalline and noncrystalline regions is at least 1:39 or at least 4 times higher than in the HPB. However, because of the difference in crystallinities in the HPB and E/B samples, a comparison of the total fraction of branches in crystalline region yields similar numbers, namely, 6%–8% for both cases, although in the E/B sample the 8% is an upper limit. In any case, care should be taken when the partitioning of ethyl branches in two different polymers is compared. The partitioning may be influenced by several factors which vary in these samples. Such factors are the total concentration of branches, the crystallinity, the polydispersity, and a possible difference in branch distribution.[16,43] Although the crystal thickness was not measured in the E/B sample, it is probable that the ratio of average branch-free stem length to crystal stem length also differed in the two samples and might affect the partitioning.[21] More work needs to be done to sort out these effects.

We can speculate whether the crystalline ethyl branches occupy interstitial positions or larger defect sites. Two observations favor the latter view. First, there is no evidence of a sharp resonance in either the methyl or the methine regions of the spectrum. A sharp resonance similar in line width to the 32.9 ppm backbone resonance would be expected if the ethyl branch were rigidly held in a particular conformation of lowest energy in the lattice. Second, the attenuation behavior of the 12.3 ppm $1B_2$ resonance in the Hartmann–Hahn mismatch experiment is comparable to the behavior of the backbone noncrystalline carbons. It follows that the local fields around these $1B_2$ carbons are probably consistent with a considerable molecular mobility in spite of the fact that these branches are found in crystalline regions. In the same way, the noncrystalline $1B_2$ carbons clearly see a smaller local field than their backbone counterparts, judging by the greater attenuation of the former carbons.

An interesting question involves the location of branches and whether branches tend to accumulate at the crystal/noncrystal interface. Presumably, if the branches were not present, the crystals would grow thicker and the lattice parameters would resemble those in linear PE. On the other hand, it has been pointed out that the interface is the region where, when one has a reasonably high molecular weight, one finds a lot of steric interference as chains make the transition from ordered to disordered conformations. The steric forces are strong enough to force a sizable fraction of stems into becoming connected by tight loops.[52] It seems reasonable that the existence of a branch at the interface would only aggravate this steric problem with the result that the branch carbons might well be forced away from the interface and deeper into the noncrystalline region. Given these conflicting ideas, we start with no particular bias as to whether the branches are concentrated at the interface.

With respect to the question of the uniformity of branch distribution in the noncrystalline region, we have noted in a previous paper that among the three CP experiments used for isolating the pure spectra, only the CP spectrum is characterized by a rather uniform proton polarization in all regions. The other two spectra are generated in the presence of significant proton polarization gradients so that different parts of the same phase contribute unequally to the resonance of that phase. Therefore, on the one hand, the technique would not be expected to work well if defects were concentrated near an interface and not distributed uniformly throughout the phase. Conversely, a uniformity of defect resonance amplitudes in each of the three linear-combination spectra used for generating each pure spectrum implies a reasonable degree of uniformity in the defect distributions within a phase. The deviation in $1B_2$ amplitudes in each of the three linear-combination spectra corresponding to the pure noncrystalline spectrum was ±9% and ±2% respectively for those sets obtained with a 1- and 3-ms (see below) CP time. It would seem very unlikely that such good agreement could be obtained if the ethyl branches were concentrated at the interface.

The distribution of ethyl branches in the crystalline region is perhaps a more interesting question. The criterion applied in the foregoing paragraph was more difficult to employ for the crystalline phase because the intensity of the crystalline $1B_2$ resonance at 12.3 ppm was quite weak, and this resonance became distorted quickly if the 11.3 ppm resonance did not null exactly in each pure crystalline linear-combination spectrum. The best indication that the branch distribution is reasonably uniform throughout the crystalline region is the $T_{1\rho}^{H}$ behavior of the 12.3 ppm resonance in the Hartmann–Hahn mismatch experiment where the observed $T_{1\rho}^{H}$ matched that of the entire crystalline phase (as detected by CP via the backbone carbon resonances). If the branches were concentrated near the interface, they would have been expected to have a $T_{1\rho}^{H}$ intermediate between the crystalline and noncrystalline values. Since some precision in the $T_{1\rho}^{H}$

measurement for the 12.3 ppm peak is lacking, this claim of a uniform distribution emphasizes not so much the uniformity of the distribution as a denial of the statement that all of the branches are to be found very close to the interface. This is particularly important because we recognize that in our definition of crystallinity, based on resonance position only, about 35% of these so-called crystalline carbons have T_1^C values which are in the range of 1–20 s. It is not yet a settled issue whether the relaxation of these carbons expresses an intrinsic mobility or whether these carbons are coupled by carbon–carbon spin exchange[42,43,53] to noncrystalline carbons. The truth very likely lies somewhere in between. It is not even known whether these carbons with shorter relaxation reside near the interface. The chemical shift of these faster relaxing carbons probably implies that their average conformation is very close to all-trans and that they are surrounded by a close to orthorhombic unit cell (as opposed to a monoclinic unit cell which has a distinct chemical shift).[54] In that sense it is reasonable that these carbons should be called crystalline. What is being claimed about the $1B_2$ carbons at 12.3 ppm is that the $T_{1\rho}^H$ sensed by these carbons is the same as that sensed by *the entire collection* of backbone carbons resonating at 32.9 ppm, including all of the sites with possibly different mobilities. In that context we claim that the branches are not likely to be clustered near the interface.

The CP method used in this study is based on assumptions that are not necessarily valid, particularly in a sample like the HPB which has a large noncrystalline content. Therefore, in the Appendix we discuss some of these matters and summarize a few experiments intended to explore the validity of the assumptions made. From an NMR point of view one would like the spin physics to be better defined in the set of CP experiments in order to carry out the branch analysis. If it were only these CP experiments that determined the confidence which we had in these results, we would be much less confident. The existence of the chemically shifted $1B_2$ resonance at 12.3 ppm was an important observation. Also our ability to verify this resonance assignment, deduced from the pure crystalline spectrum, by an identification of this line with the crystalline $T_{1\rho}^H$ was also significant. Finally, there is an underlying assumption which is reasonable on physical grounds, namely, that the branches included in the crystalline domains should be less mobile, should experience stronger dipolar interactions, and should, therefore, have carbon resonances which, after 1 ms of CP, are much more quantitative and much easier to interpret. Thus, if one has two spectrally resolved components, one well-behaved and one not so well-behaved in CP, one can still extract the true partitioning from the CP experiments by interpreting the well-behaved resonance quantitatively and deducing the other's concentration by difference with respect to the known average concentration. Therefore, while we are not totally confident about the spin physics in the noncrystalline region, we are still confident about these results.

Acknowledgment. E. P. acknowledges the Research Council of Spain (CSIC) for the award of a research grant that supported this work at the National Bureau of Standards. The synthesis and characterization of HPB was funded by the NSF–MRL program through Northwestern's Materials Research Center (DMR82-16972).

Appendix

With respect to the NMR method for separating ethyl branch resonances into their crystalline and noncrystalline components, a fundamental premise was that proton spin diffusion over distances of, say, 0.5 nm, be reasonably effective on the time scales of the CP time and the fastest intrinsic $T_{1\rho}^H$ in the system, i.e., about 1 ms in this case. The presence of magic-angle spinning (MAS) can, in principle, suppress spin diffusion. This is a matter of concern for PE, particularly in the noncrystalline regions since spinning sidebands in the proton spectrta have been observed at a spinning speed of 2 kHZ and above.[55] The presence of sidebands implies that the MAS is averaging the dipolar interactions, thereby, suppressing spin diffusion. A side group which has additional degrees of freedom to reorient its bond vectors will probably see an even weaker dipolar field than its noncrystalline backbone counterparts with the result that MAS might be even more effective in quenching spin diffusion.

A second matter of concern is the homogeneity of each phase with respect to intrinsic relaxation times and CP efficiencies. If, for example, a given domain contained substantially different mobilities separated on a distance scale larger than 1 nm, then, within such a domain, CP efficiency differences would likely exist as well as possible differences in $T_{1\rho}^H$ behavior. This situation would undermine the two-phase analysis. It has been noted in the literature[44] that the noncrystalline PE backbone carbons have uniform T_1^C values, yet they have two transverse relaxation time (T_2^C) values. Since this latter parameter, because of the way it is measured, is determined to a large degree by residual local proton dipolar fields, the multiple T_2^C values have been taken to indicate the presence of regions of different mobilities within the noncrystalline region. Furthermore, the interpretation given to the multiple T_2^C's was that the shorter T_2^C component corresponds to the more constrained noncrystalline interface carbons. If the noncrystalline region consists of layered regions of varying mobility, then our method may run into trouble. On the other hand, if mobility variations exist, mixed on an intimate scale (less than 1 nm), the two-phase analysis will still give reasonable results.

Several auxiliary experiments were undertaken in order to examine the validity of the method and to expose possible ill effects of MAS and large-scale motional heterogeneity within the two phases. The entire set of experiments is too large to report in detail, so only a few summary statements will be given. Both ^{13}C and ^1H observation were employed in these experiments.

First, the CP procedure for determining partitioning was repeated at a spinning speed of 0.77 kHz and a CP time of 1 ms. The spectral separation of the 11.3 and the 12.3 ppm peaks as well as the apparent $1B_2$ concentrations in the pure crystalline and pure noncrystalline spectra were in excellent agreement with the results at a spinning speed of 3.2 kHz (see Figure 4). Therefore, the rate of MAS does not seem to interfere with spin diffusion to the extent of affecting the results. To have comparable CP efficiencies in the presence of proton sidebands is not unreasonable so long as the strengths of the proton and carbon ratio frequency fields are adjusted to optimize the CP process at a given spinning frequency.[33]

Second, at a spinning speed of 3 kHz, an extension of the CP time to 3 ms with the same set of experiments gave apparent ethyl branch concentrations of 3.4 ± 0.7 and 27.0 ± 1.5 per thousand total carbon atoms in the crystalline and noncrystalline regions, respectively. These concentrations are much closer to the true concentrations, which were deduced in the Results section. Improved agreement by use of a 3-ms CP time could be predicted from Figure 6 and CP theory,[56] assuming that the carbons were not

relaxing to the lattice during CP and that the noncrystalline region was characterized by a single CP rate constant and a single intrinsic $T_{1\rho}^{H}$. The CP intensities of the noncrystalline backbone carbons, against which the noncrystalline $1B_2$ intensity is normalized, do not, however, support the validity of these assumptions. Therefore, this excellent agreement becomes somewhat fortuitous.

Third, the behavior of the noncrystalline proton resonance is as follows: The nonspinning line width is 4600 Hz, but this line shape is neither Lorentzian nor Gaussian. In fact, this noncrystalline line could be the superposition of two lines of widths 3 and 10 kHz with approximate intensity ratio 1:3. Spinning sidebands can be seen already at 1-kHz spinning speed. The sideband intensities increase with spinning speed, indicating that a greater and greater fraction of the noncrystalline protons are being averaged by MAS. For example, at a 2.8-kHz spinning speed, there is a narrowed portion of the noncrystalline line (with sidebands) and a 10-kHz-wide portion (no sidebands). The ratio of these components is about 1:0.85. The narrowed centerband has a line width of about 400 Hz regardless of spinning speed; however, the centerband shows a monotonic increase in intensity with spinning speed. Therefore, line narrowing is a continuous process, and there is no indication of a bimodal distribution of mobility. The line narrowing behaves more like there is a continuum of dipolar interactions in the static sample and that these interactions are not all averaged at once. Such a continuum might well arise from a distribution of angles of motional constraint (with respect to the static field direction). Judging by the line width, the static proton interaction is already reduced by motion about 15-fold.

Fourth, proton signals were directly observed by using the MAS probe in an experiment in which the protons were prepared by the "DE5" sequence, followed by an immediate restoration of the proton magnetization along the static field and a variable delay time before observation. The DE5 sequence selected a slightly smaller relative fraction (0.38) of the broader, 10-kHz-wide, noncrystalline component, compared with the corresponding fraction (0.46) in the equilibrium line shape. This selection of narrower lines is consistent with expectations for the response to a dipolar echo in the presence of MAS. It then took at least 15 ms of spin diffusion before the noncrystalline line shape returned to its equilibrium shape. Such a slow recovery of shape means that there are probably regions of differing local fields which are segregated in space on a scale of 1–2 nm, or the spins showing strong spinning sidebands are really in very poor spin-diffusion contact with the other protons, even though they are rather well-mixed through the matrix. The former interpretation, i.e., spatial segregation, is supported by the observation that the restoration of the equilibrium noncrystalline shape is similarly slow for a static sample following a T_2^{H} selective preparation and a spin-diffusion period. A final comment about this experiment is that the behavior of the broader noncrystalline fraction during the spin-diffusion period is not consistent with expectations based on assigning this broader component to the crystal/noncrystal interface. In that sense the results are interesting. We may report on this in another publication. We emphasize again, however, that while the foregoing description is cast in terms of two noncrystalline components, this is merely a matter of convenience since the fractions of the two components depend on spinning speed.

Fifth, T_2^{C} values were measured for the various carbons. In our sample, the decay of the noncrystalline backbone carbon magnetization could be adequately decomposed into two T_2^{C} values, 0.05 and 1.2 ms. The 11.3 ppm $1B_2$ peak only had one T_2^{C}, also about 1.2 ms; however, the methine peak had a similar behavior to the noncrystalline backbone resonance. Interestingly, the fraction of the longer T_2^{C} was very dependent on the spinning frequency, as one would expect if there was a continuum of dipolar fields as the proton results suggest. Actually, the measurement of T_2^{C} in the presence of MAS is not as well-defined as one would like since some echo formation is expected at the end of each rotor period. Such periodicity is present, although it is a weak effect; ideally, sampling should be restricted to intervals having integral rotor periods. The measurements cited above did not obey such restrictions. Nevertheless, it is very clear that the decays do not fit an exponentially damped set of rotational echoes. An apparent heterogeneity of local fields seems to exist.

Taken together, the five foregoing observations generally support the CP method for separating resonances belonging to the two PE phases in that the CP results do not seem to depend on the choice of spinning speed. The existence of noncrystalline sites of differing dipolar field strength seems to be clear, although there does not seem to be a bimodal distribution so much as a continuum of local fields. This continuum may well reflect an orientation dependence to the direction of residual constraint in already highly averaged interactions. (The latter strong averaging leads to the uniform T_1^{C} values in the noncrystalline region.) Thus, the differences in local dipolar fields need not immediately imply a difference in mobility, although there are indications that the protons which see different fields are clustered into domains which may be in the 1–2-nm size range. At the same time, none of the three preparation sequences for the proton showed an overwhelming preference for wider or narrower noncrystalline lines, and perhaps that is why the separation of crystalline and noncrystalline branch resonances was quite consistent. The other concept which would help to explain the consistent results using the two-phase analysis is that these smaller domains of varying local field probably are not stratified with respect to the lamellar surface. Thus, spin diffusion, on average, might progress uniformly through the noncrystalline region with the result that the heterogeneity of this domain becomes more obscured. A warning is clearly in order, however, since spinning speeds within the realm of today's technology could probably be achieved that would quench spin diffusion to such an extent that this analysis would fail.

In any case, the HPB, with its very large noncrystalline fraction and rather narrow noncrystalline proton line width, represents one of the least favorable cases for the application of this partitioning method to PE, and, except for the intensity distortions, the method works exceedingly well for the choice of experimental conditions used herein.

References and Notes

(1) Flory, P. J. *Trans. Faraday Soc.* **1955**, *51*, 848.
(2) Killian, H. G. *Colloid Polym. Sci.* **1984**, *262*, 374.
(3) Holdsworth, P. J.; Keller, A. *J. Polym. Sci., Part B* **1967**, *5*, 605.
(4) Kawai, T.; Kozaburo, U.; Maeda, H. *Makromol. Chem.* **1970**, *132*, 87.
(5) Cole, E. A.; Holmes, D. R. *J. Polym. Sci.* **1960**, *46*, 147.
(6) Swan, P. R. *J. Polym. Sci.* **1962**, *56*, 409.
(7) Baker, C. H.; Mandelkern, L. *Polymer* **1966**, *7*, 71.
(8) Shirayama, K.; Kita, S.; Watabe, H. *Makromol. Chem.* **1972**, *151*, 97.
(9) Vonk, C. G. *J. Polym. Sci., Part C* **1972**, *38*, 429.
(10) Preedy, J. E. *Br. Polym. J.* **1973**, *5*, 13.
(11) Martuscelli, E. *J. Macromol. Sci., Phys.* **1975**, *B11*, 1.
(12) Balta Calleja, F. J.; Gonzalez Ortega, J. C.; Martinez de Salazar, J. *Polymer* **1978**, *19*, 1094.

(13) Balta Calleja, F. J.; Hosemann, R. *J. Polym. Sci., Polym. Phys. Ed.* **1980**, *18*, 1159.
(14) Richardson, M. J.; Flory, P. J.; Jackson, J. B. *Polymer* **1963**, *4*, 221.
(15) Bunn, C. W. In *Polyethylene*; Renfrew, A.; Morgan, P., Eds.; Illife: London, 1957; Chapter 5.
(16) Alamo, R.; Domszy, R. C.; Mandelkern, L. *J. Phys. Chem.* **1984**, *88*, 6587.
(17) Keller, A.; Priest, D. J. *J. Macromol. Sci., Phys.* **1968**, *B2*, 479.
(18) Keller, A.; Priest, D. J. *J. Polym. Sci., Part B* **1970**, *8*, 13.
(19) Witenhafer, D. E.; Koenig, J. L. *J. Polym. Sci., Polym. Phys. Ed.* **1969**, *7*, 1279.
(20) Runt, J.; Harrison, I. R. *J. Polym. Sci., Polym. Phys. Ed.* **1978**, *16*, 375.
(21) Vonk, C. G.; Pijpers, A. P. *J. Polym. Sci., Polym. Phys. Ed.* **1985**, *23*, 2517.
(22) Vile, J.; Hendra, P. J.; Wilis, H. A.; Cudby, M. E. A.; Bunn, A. *Polymer* **1984**, *25*, 1173.
(23) Holdsworth, P. J.; Keller, A. *Makromol. Chem.* **1969**, *125*, 82.
(24) Domszy, R. C.; Alamo, R.; Mathieu, P. J. M.; Mandelkern, L. *J. Polym. Sci., Polym. Phys. Ed.* **1984**, *22*, 1727.
(25) Vanderhart, D. L.; Pérez, E. *Macromolecules* **1986**, *19*, 1902.
(26) Pines, A.; Gibby, M. G.; Waugh, J. S. *J. Chem. Phys.* **1973**, *59*, 569.
(27) Sarles, L. R.; Cotts, R. M. *Phys. Rev.* **1958**, *111*, 853.
(28) Andrew, E. R. *Prog. Nucl. Magn. Reson. Spectrosc.* **1972**, *8*, 1.
(29) Lowe, I. J. *Phys. Rev. Lett.* **1959**, *2*, 85.
(30) Schaefer, J.; Stejskal, E. O.; Buchdahl, R. *Macromolecules* **1975**, *8*, 291.
(31) Garroway, A. N.; Moniz, W. B.; Resing, H. A. *Coat. Plast. Prepr. Pap. Meet. (Am. Chem. Soc., Div. Org. Coat. Plast. Chem.)* **1976**, *36*, 133.
(32) Certain commerical companies are named in order to specify adequately the experimental procedure. This in no way implies endorsement or recommendation by NBS.
(33) Stejskal, E. O.; Schaefer, J. *J. Magn. Reson.* **1977**, *28*, 105.
(34) Randall, J. C. In *Polymer Characterization by ESR and NMR*; ACS Symposium Series 142; Woodward, A. E., Bovey, F. A., Eds.; American Chemical Society: Washington, DC, 1980.
(35) Rachapudy, H.; Smith, G. G.; Raju, V. R.; Graessley, W. W. *J. Polym. Sci., Polym. Phys. Ed.* **1979**, *17*, 1211.
(36) Randall, J. C. *J. Polym. Sci., Polym. Phys. Ed.* **1975**, *13*, 1975.
(37) Krigas, T. M.; Carella, J. M.; Strujlinski, M. J.; Crist, B.; Graessley, W. W.; Schilling, F. C. *J. Polym. Sci., Polym. Phys. Ed.* **1985**, *23*, 509.
(38) Crist, B.; Graessley, W. W.; Wignall, G. D. *Polymer* **1972**, *23*, 1561.
(39) Howard, P. R. Ph.D. Thesis, Northwestern University, 1986.
(40) Noggle, J. H.; Schirmer, R. E. In *The Nuclear Overhauser Effect*; Academic: New York, 1971.
(41) Torchia, D. A. *J. Magn. Reson.* **1978**, *30*, 613.
(42) Axelson, D. E.; Mandelkern, L.; Popli, R.; Mathieu, P. *J. Polym. Sci., Polym. Phys. Ed.* **1983**, *21*, 2319.
(43) Axelson, D. E. *J. Polym. Sci., Polym. Phys. Ed.* **1982**, *20*, 1427.
(44) Kitamaru, R.; Horii, F.; Murayama, K. *Macromolecules* **1986**, *19*, 636.
(45) Schröter, B.; Posern, A. *Makromol. Chem., Rapid Commun.* **1982**, *3*, 623.
(46) Axelson, D. E.; Levy, G. C.; Mandelkern, L. *Macromolecules* **1979**, *12*, 41.
(47) (a) Dorman, D. E.; Otocka, E. P.; Bovey, F. A. *Macromolecules* **1972**, *5*, 574. (b) Bovey, F. A.; Schilling, F. C.; McCrackin, F. L.; Wagner, H. L. *Macromolecules* **1976**, *9*, 76.
(48) Usami, T.; Takayama, S. *Macromolecules* **1984**, *17*, 1756.
(49) Ostroff, E. D.; Waugh, J. S. *Phys. Rev. Lett.* **1966**, *16*, 1097.
(50) Seguela, R.; Rietsch, F. *J. Polym. Sci., Polym. Lett. Ed.* **1986**, *24*, 29.
(51) Laupetre, F.; Monnerie, L.; Barthelemy, L.; Vairon, J. P.; Sauzeau, A.; Roussel, D. *Polym. Bull. (Berlin)* **1986**, *15*, 159.
(52) Guttman, C. M.; DiMarzio, E. A.; Hoffman, J. D. *Polymer* **1981**, *22*, 1466.
(53) VanderHart, D. L., to be published.
(54) VanderHart, D. L.; Khoury, F. *Polymer* **1984**, *25*, 1589.
(55) Schneider, B.; Pivocova, H.; Doskocilova, D. *Macromolecules* **1972**, *5*, 1589.
(56) Garroway, A. N.; Moniz, W. B.; Resing, H. A. *Carbon-13 NMR in Polymer Science*; ACS Symposium Series 103; W. M. Pasika, Ed.; American Chemical Society: Washington, DC, 1979.

Small-Angle Scattering of the Statistical Structure of Domain Boundaries

W. Ruland

Fachbereich Physikalische Chemie, Bereich Polymere, Universität Marburg, D-3550 Marburg/Lahn, F.R.G. *Received June 9, 1986*

ABSTRACT: The determination of the width of domain boundaries by the SAXS method can contain substantial errors if the boundary region is not represented by a smooth homogeneous density transition but by a statistical structure of a certain coarseness. It is shown that these errors lead, in general, to an underestimation of the values of the boundary widths and to a compensation of the expected increase of these values with temperature in the case of block copolymers. SAXS studies of samples with a high preferred orientation of the interface planes can be used to minimize the errors and to obtain information on the coarseness of the statistical structure of the domain boundaries.

Introduction

The width of domain boundaries is an important parameter for the characterization of microphase separation in polymers. By use of small-angle X-ray scattering, this parameter is obtained by measurements in the range of validity of Porod's law.[1-8] In this range, the correct subtraction of the background is essential for an accurate determination of the boundary width, especially in the case of slit-smeared intensities.[6]

The theory of microphase separation in block copolymers[9-11] predicts the relationship

$$d_z = 2\langle a \rangle / (6\chi)^{1/2} \quad (1)$$

where d_z is the boundary width, χ the Flory–Huggins interaction parameter, and $\langle a \rangle$ the average length of a monomer unit. Consequently, measurements of d_z as a function of temperature could, in principle, be used to determine the temperature dependence of χ.

SAXS measurements carried out by Roe, Fishkis, and Chang[5] on block copolymer melts did not, however, show the decrease of the intensity at large scattering angles predicted by the temperature dependence of d_z according to eq 1. This observation was confirmed by similar measurements carried out in my research group, the details of which will be reported in a separate paper. Furthermore, the d_z values determined for block copolymers at room temperature were found to be significantly smaller than the theoretically predicted ones.[6] The aim of this paper is to investigate the possibility of an influence of the statistical structure of the domain boundaries on the de-

0024-9297/87/2220-0087$01.50/0